

## Imaging through gas-filled sediments using marine shear-wave data

John R. Granli\*, Børge Arntsen\*, Anders Sollid\*, and Eilert Hilde\*

### ABSTRACT

Marine multicomponent sea-floor data of excellent quality have been acquired over the Tommeliten Alpha field. The most dominating wave modes are interpreted to be conventional compressional *PP*-waves and converted *PS*-waves. The most important geophysical problem associated with the Tommeliten Alpha field is the presence of a gas chimney obscuring the conventional 3-D seismic image of the reservoir zone. The converted *PS*-waves effectively undershoot the gas chimney, leading to substantially improved images of the reservoir. Subsequent interpretation indicates the Tommeliten Alpha structure is a faulted dome.

### INTRODUCTION

The Tommeliten chalk fields Alpha and Gamma are located in the southern North Sea. They consist of two diapiric structures, 10 km apart, that contain hydrocarbons in chalk of Late Cretaceous and early Paleocene age. The water depth in the area is approximately 70 m, and the areal extent is 7 km<sup>2</sup> for Alpha and 4.5 km<sup>2</sup> for Gamma. Figure 1 shows a seismic profile over the Alpha structure. The reservoir is located in the Ekofisk Formation at a depth of approximately 3 km. A slightly deeper reservoir, the Tor Formation, has the same polarity as Ekofisk and is located approximately 60 ms below Top Ekofisk.

From Figure 1 we observe that the seismic data quality is clearly severely deteriorated in a zone approximately 2 km wide extending from the top of the Ekofisk Formation and almost up to the surface. A possible explanation for the bad data quality is gas leakage from the reservoir into the overlying sediments. It is well known (e.g., White, 1975) that presence of gas in the subsurface has a strong effect on compressional waves. The reason for this is that the bulk modulus, defined by degree of resistance against rock compression and an important

constituent in the definition of compressional-wave velocity, is severely distorted. Only small amounts of gas will seriously affect both traveltime and reflection amplitude for compressional waves. Unfortunately, seismic processing can only marginally compensate for this effect.

Figure 2 shows a contour map of the Tommeliten Top Ekofisk horizon. The black hole in the middle of Figure 2 shows the areal extent of the Top Ekofisk Formation where these data, because of gas distortion, provide no structural information about the geology. Resolving this imaging problem has been the main geophysical challenge since the Alpha discovery in 1977. Compressional-wave undershooting based on conventional acquisition with a compressional-wave source and marine streamer, using very large offsets, has been attempted at several locations in the southern North Sea (Dangerfield, 1992), but no breakthrough for the imaging problems beneath gas has been seen so far.

Gas usually has a small effect on the rock density and no significant effect on shear modulus, loosely defined by degree of resistance against rock deformation and the main constituent in shear-wave velocity. Hence, shear waves are much less affected by gas than compressional waves. The potential for use of shear-wave data to image through gas has been shown by Berg et al. (1994a,b). However, the work was based on the assumption that compressional waves were converting to shear waves at the sea floor and then propagating as pure shear waves down to the target and up again to the sea floor.

We show in the present study that the most important shear-wave mode observed in marine multicomponent data from the Tommeliten field is in fact compressional waves converted to shear waves at the target. We also show that converted waves can be used successfully for imaging through a gas chimney, provided that the asymmetrical nature of the converted wave raypath is taken into account. Finally, the excellent data quality of marine multicomponent sea-floor data is demonstrated.

Processing and interpretation of converted wave modes are well described in the literature. We build on the results of

Presented at the 65th Annual International Meeting, Society of Exploration Geophysicists. Manuscript received by the Editor June 23, 1997; revised manuscript received October 1, 1998.

\*Statoil, Arkitekt Ebbells veg 10, 7005 Trondheim, Norway. E-mail: barn@statoil.no.  
© 1999 Society of Exploration Geophysicists. All rights reserved.

Tessmer and Behle (1988) and Tessmer et al. (1990) for stacking of converted waves, and Harrison (1992) and Harrison and Stewart (1993) for dip moveout (DMO) and poststack migration of converted waves.

The paper is organized as follows: The first section contains a review of data acquisition geometry and a discussion of major wave modes present in the data. Processing of the multicomponent sea-floor data is discussed in the second section, while a geological interpretation is attempted in the third section.

### MARINE MULTICOMPONENT DATA ACQUISITION AND MODE IDENTIFICATION

Multicomponent marine data acquisition is a two-boat operation with sensors located at the sea floor as illustrated in Figure 3. Each sensor contains a three-component geophone measuring particle velocity and a hydrophone measuring pressure in the water. The sensor is planted into the sea floor by a remotely operated submarine. Orientation and tilt of the components are measured relative to a fixed coordinate system by built-in compasses and inclinometers. The seismic source used in the Tommeliten case was a conventional marine air gun array, towed at around 6 m water depth. The data were digitized and transmitted to the receiver vessel via a cable connection.

During operation at Tommeliten, the source initially was positioned at the maximum 4.5-km offset from the receiver array. Then 325 successive shots at 28 m spacing were fired along the traverse shown in Figure 2. In total that amounted to 9 km recording offset, 4.5 km on each side of the sensor array. When the source boat was finished with one sequence (sail line), the sensors were towed to the next location, approximately 112 m up the line, and the experiment was repeated. A total of 1484 common receiver gathers at 7 m spacing were acquired during the field experiment.

The geophone measures horizontal in-line, horizontal cross-line, and vertical particle velocities; the hydrophone measures pressure in the water. Hereafter these components will, for simplicity, be denoted as  $X$ ,  $Y$ ,  $Z$ , and  $P$ , respectively.

Figure 4 displays the common receiver gathers recorded at two subsequent sensors, located to the south of the Alpha structure. The most striking feature is the band of strong events recorded between 6 and 7 s at the  $X$ -component, which is hardly visible at the  $Y$ -component. The vertical  $Z$ -component and the hydrophone component record a similar band of events but at the much earlier time—between 3 and 3.5 s.

Figure 5 shows the result of ray tracing in a simplified depth model of a part of the Tommeliten field. The raypaths illustrate the wave modes expected to be present in the recorded data. Particularly note the modes denoted by  $SS$  and  $PS$ . The former is a compressional wave converting to a shear wave in the sea floor and then propagating down to the target reflector and up again to the sea floor. The latter is a compressional wave

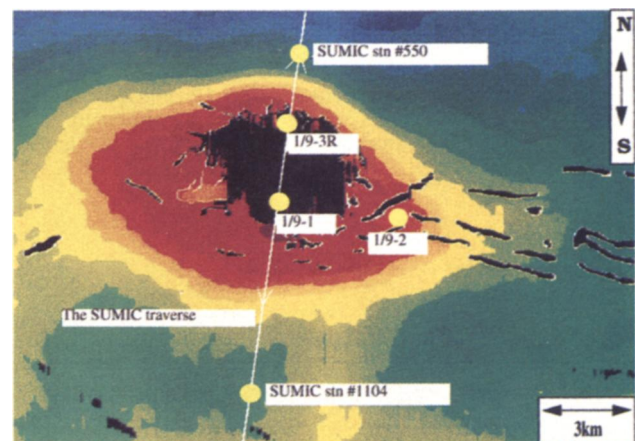


FIG. 2. Contour map showing the Tommeliten Top Ekofisk horizon. Red corresponds to shallow areas, green denotes deep areas, and black represents areas where interpretation was impossible because of bad data quality. The multicomponent sea-floor data were acquired along the line labeled as the Sumic traverse.

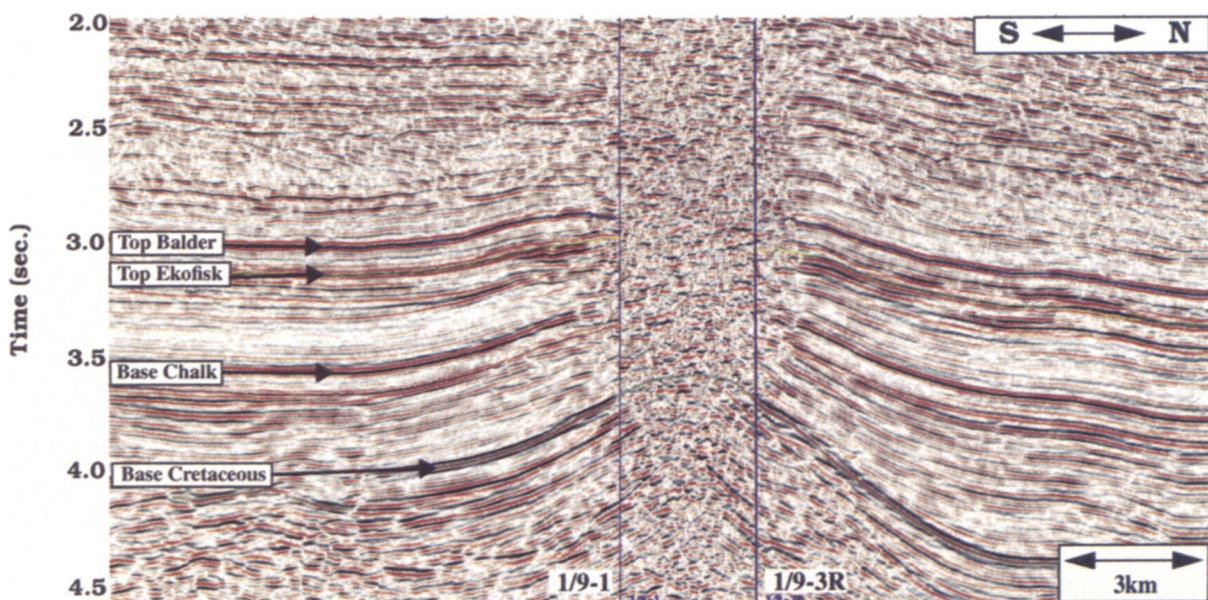


FIG. 1. Conventional 3-D random line showing the Tommeliten Alpha structure and the locations of well 1/9-1 and 1/9-3R.

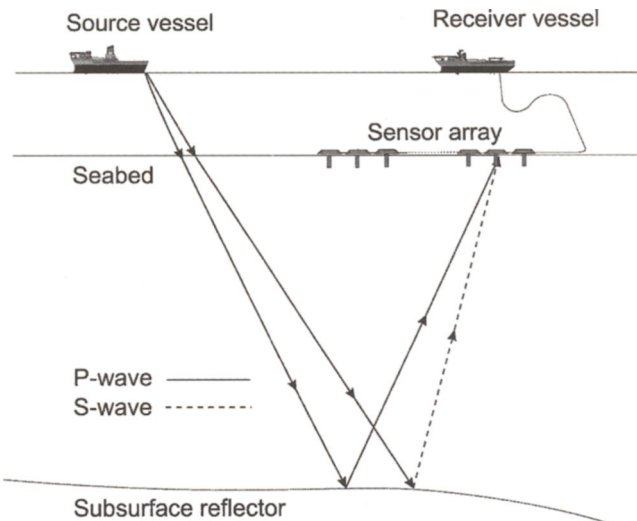


FIG. 3. Marine multicomponent sea-floor data acquisition geometry. The receiver vessel is stationary and connected to the receiver (sensor) array during the acquisition of each common receiver gather.

propagating downward to the target reflector then converting to a shear wave and propagating upward to the sea floor as a shear wave. The wave mode labeled *PP* represents a pure compressional wave.

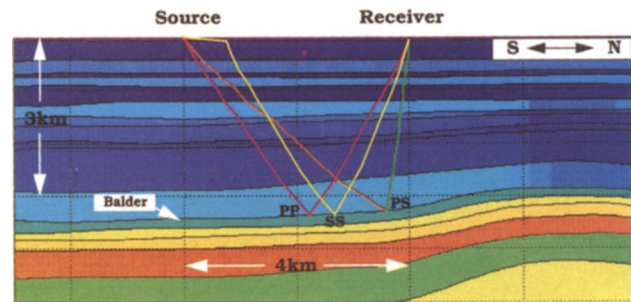


FIG. 5. Ray tracing in a simplified depth model of the Tommeliten field. The Alpha structure is located to the north (far right). Only part of the Alpha structure is shown. The raypaths show possible wave modes present in marine multicomponent sea-floor data.

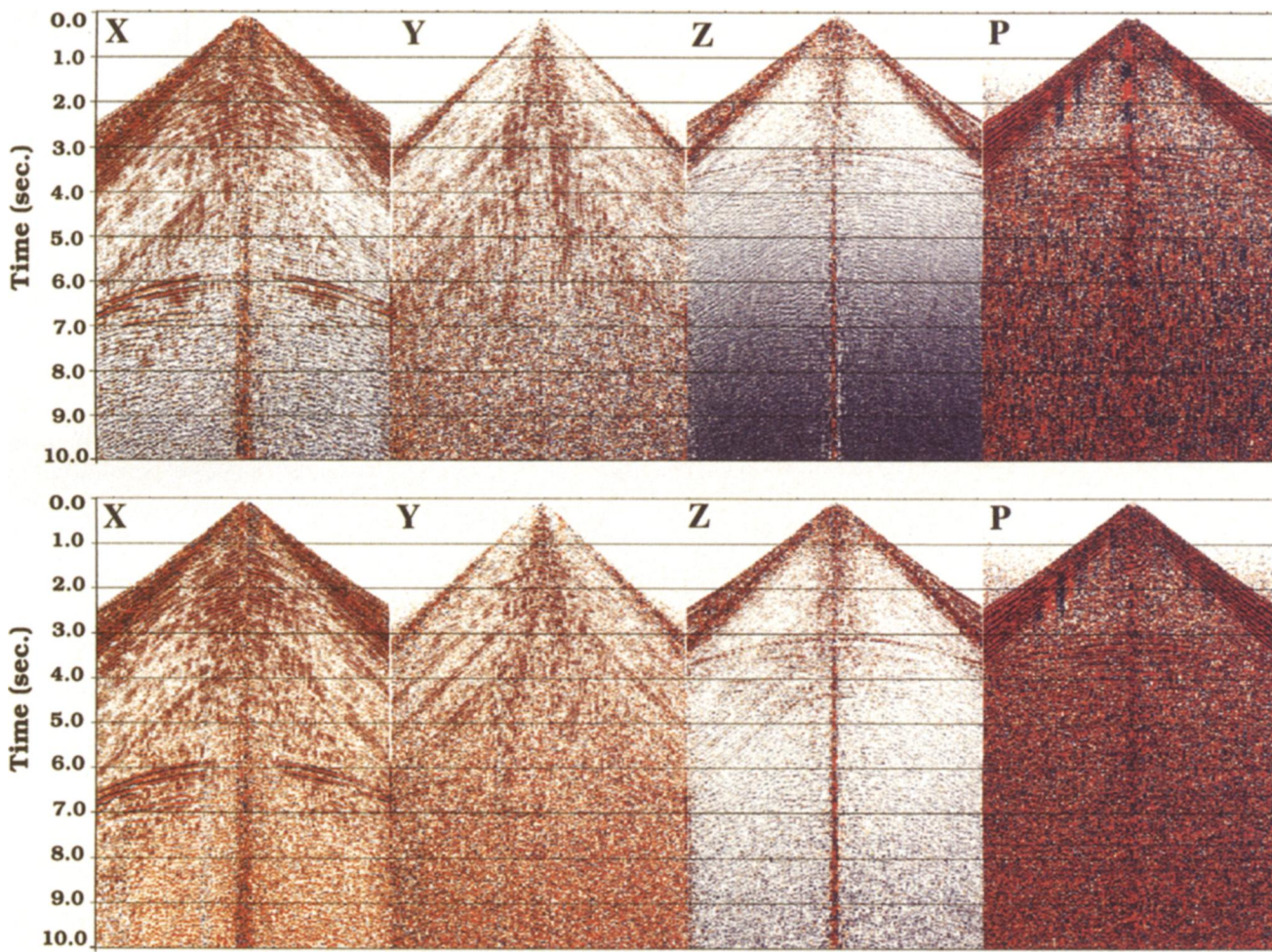


FIG. 4. Marine multicomponent sea-floor common receiver gathers at two subsequent sensors. The horizontal axis is horizontal distance (offset) away from the receiver, while the vertical axis is time.

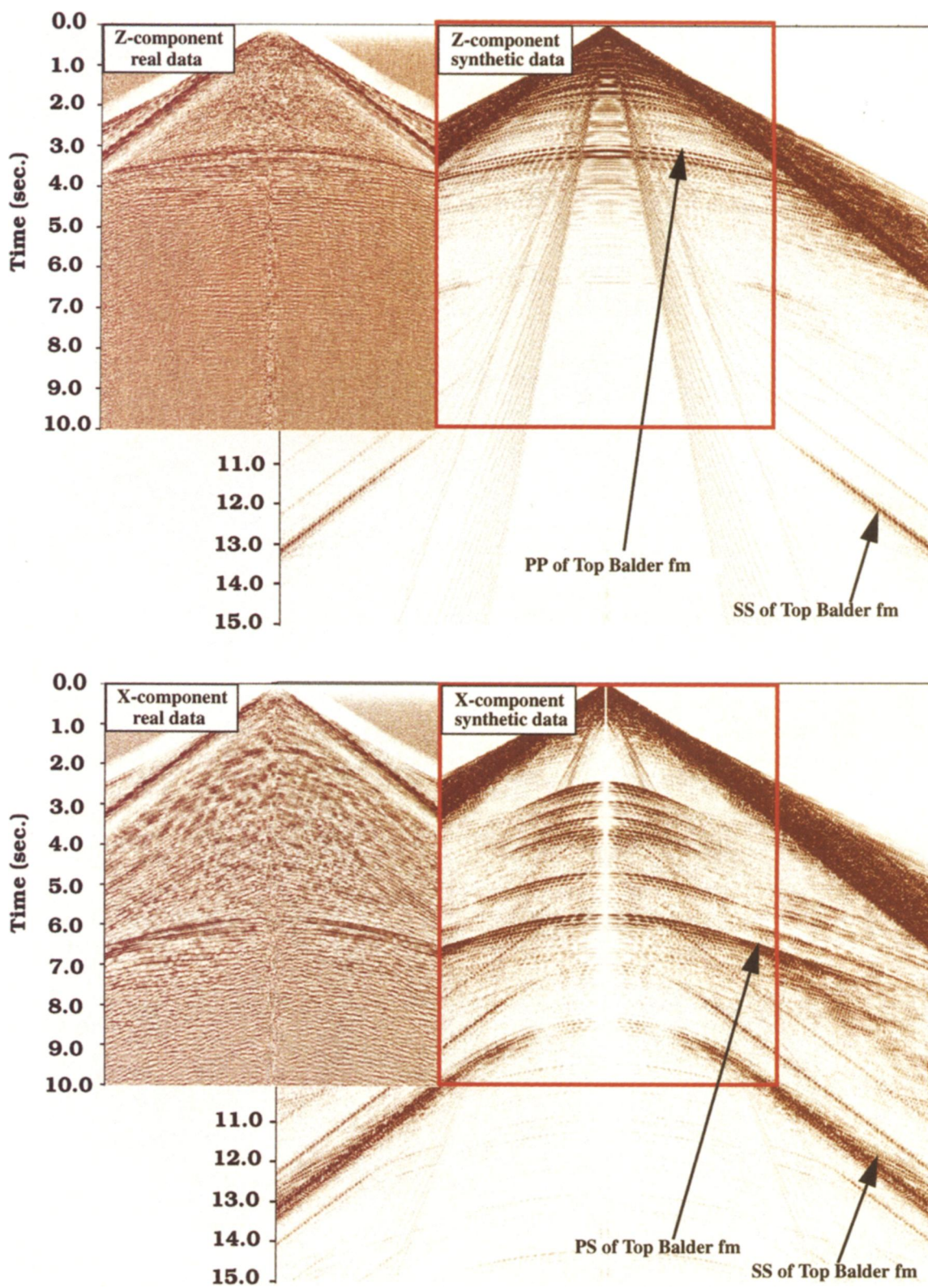


FIG. 6. Comparison between synthetic X- and Z-components of a single common receiver gather and a real common receiver gather. The red rectangles overlaying the synthetic data indicate the largest offset and largest time present in the recorded data.

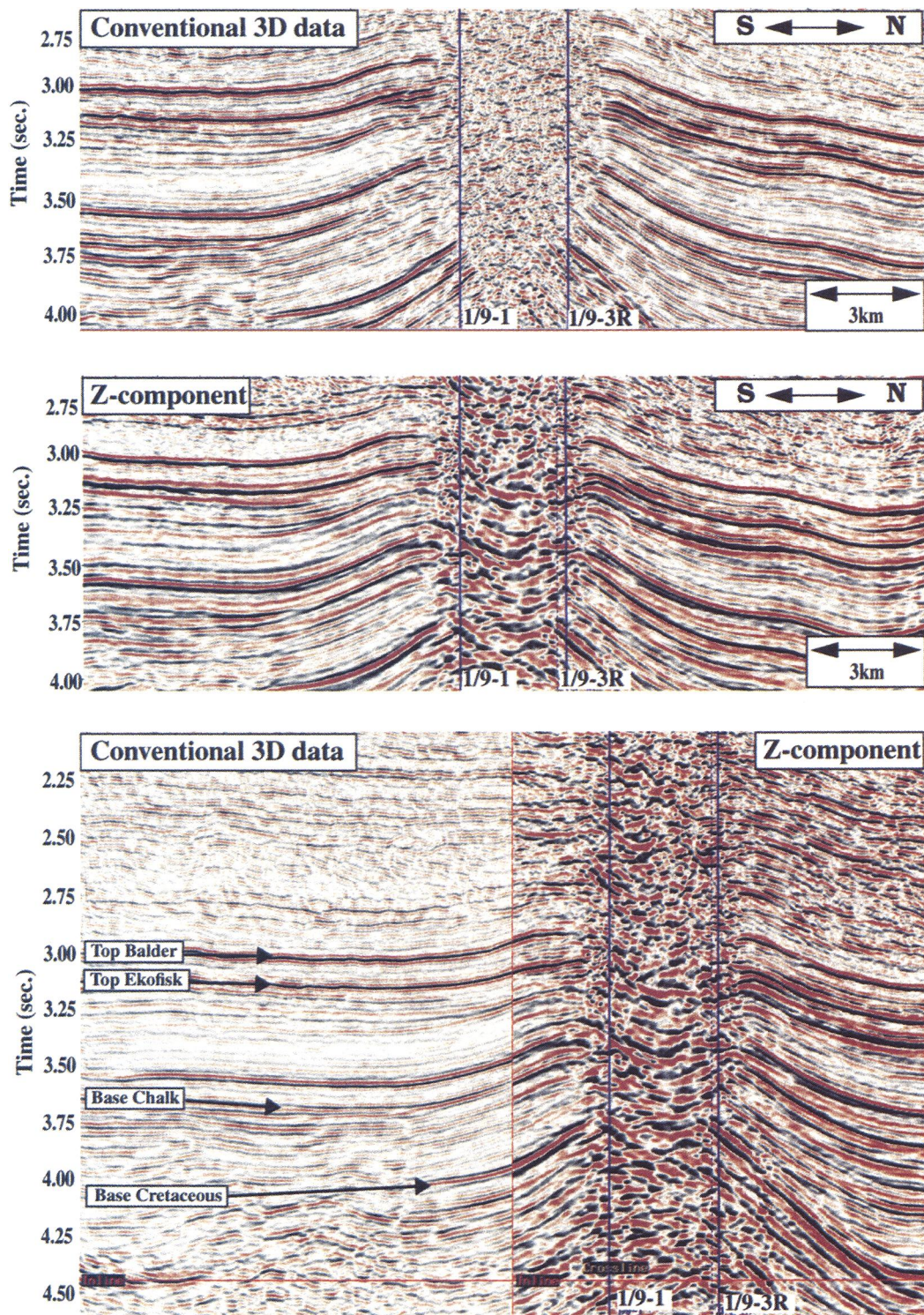


FIG. 7. Comparison of conventional 3-D data (top) and the processed Z-component (middle). The bottom section shows part of the conventional 3-D data back to back with the processed Z-component. The vertical lines indicate the well positions. The time scale of the bottom section is slightly changed to ease comparison between conventional data and the Z-component of the sea-floor data.

Because of the presence of a low shear-wave velocity zone in the vicinity of the sea floor, one would expect the Z-component to consist mainly of compressional-wave arrivals, while the X- and Y-components would be expected to contain a mixture of compressional-wave and shear-wave arrivals. The strong events between 6 and 7 s are naturally interpreted as either SS or PS events because of the rapid decrease of the amplitude with decreasing offset. The arrivals between 3 and 3.5 s on the Z-component are interpreted as PP events and are also easily identified on the conventional 3-D data.

To make a reliable interpretation of the wave modes present in the data, a full-waveform modeling program was used to generate the synthetic data shown in Figure 6. The modeling was done using a 3-D wavenumber-frequency domain approach with a simplified plane layered depth model. The compressional-wave velocity model was constructed using well logs and migration velocity analysis of the Z-component, while the shear-wave velocity model was constructed using two different approaches. At small depths, the shear-wave velocity model was derived by analyzing dispersive surface waves propagating at a slightly lower velocity than shear waves along or just beneath the sea floor (Allnor et al., 1997). The rest of the shear-wave model was estimated by a scaled version of the compressional-wave model, using a constant compressional-to-shear-wave velocity ratio. Several ratios were tried, but a compressional-to-shear-wave velocity ratio of approximately 3, as described by Dangerfield and Brown (1987), fit the observed data and was used in the final modeling shown in Figure 6.

The lower part of Figure 6 shows a comparison between the X-component of a single common receiver gather and the X-component of the synthetic data. The events indicated as PS events in the synthetic data match very nicely a set of corresponding events in the observed data. The upper part of Figure 6 shows real and synthetic data from the Z-component. The strong event at 3 s observed in the synthetic data shows a clear correlation with the corresponding event in the real data. Note the significant amount of PS-mode energy reflected from the target level, which was lost in the field as the result of insufficient offsets in the recording window. Even though SS reflections from the reservoir are clearly generated in the synthetic X-component data, they unfortunately have small relative amplitudes in the field recording window. In the real dataset it has not been possible to detect and utilize the SS energy, expected to arrive at the X-component between 9 and 10 s at zero offset.

### PROCESSING

In the present work no attempt has been made to combine the X-, Y-, Z-, and P-components into separate scalar data sets containing pure compressional and pure shear events. Amundsen and Reitan (1995) describe how multicomponent sea-floor data can be decomposed into separate up- and down-going shear and compressional data sets. Unfortunately, the data quality of the P-component was inadequate because of instrumentation problems, so the separation technique described by Amundsen and Reitan could not be used. We instead assumed the X-component contains only the PS mode and the Z-component contains only the PP mode. This is clearly an oversimplification, and one would expect compressional events

on the X-component to contribute to the PS mode images. However, because of the different propagation velocities of PP and PS modes, stacking tends to suppress PP modes in the PS images. The Y-component was not fully processed, and only a brute stack was produced.

For the PP-wave mode, conventional marine processing using the CMP principle is applicable. Note, however, that the data initially must be processed to common datum for source and receiver. Since the water layer P leg is close to vertical for both the PP and PS modes and the water layer is quite shallow (70 m), redatuming for those modes could be carried out by a vertical 48 ms time shift. This is crude but is not expected to have a significant effect on positioning and subsequent velocity analysis. The processing includes filtering, deconvolution, static time shifts, stack, and migration. Figure 7 shows the processed Z-component compared with the conventional 3-D data. The problem with imaging the area containing the gas chimney is evident and makes the interpretation of this area uncertain.

As illustrated in Figure 5, the reflection point for a PS event is not located at the midpoint between source and receiver, even for a perfectly plane reflector. This implies that a conventional processing sequence using common midpoint (CMP) sorting cannot be used. Instead, a specially adapted processing sequence as shown in a simplified form in Figure 8 is used.

The box denoted by PS-DMO in Figure 8 is a specially adapted DMO process that takes into account the asymmetry of the PS raypath (Harrison, 1992). The position of the reflection point depends in general on depth and the ratio of the compressional-to-shear-wave velocity. However, velocity analysis cannot be performed before the PS DMO process has been applied. An initial depth-dependent guess of the compressional-to-shear-wave velocity ratio based on the modeling results was then made. After application of PS DMO, a preliminary velocity analysis was made and a stack produced. The initial guess of the compressional-to-shear-wave velocity ratio was then updated by comparing the processed

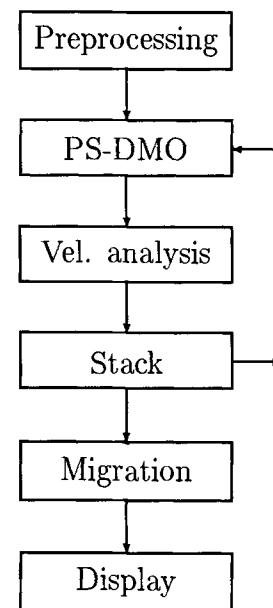


FIG. 8. Simplified PS processing sequence used to process the X-component.

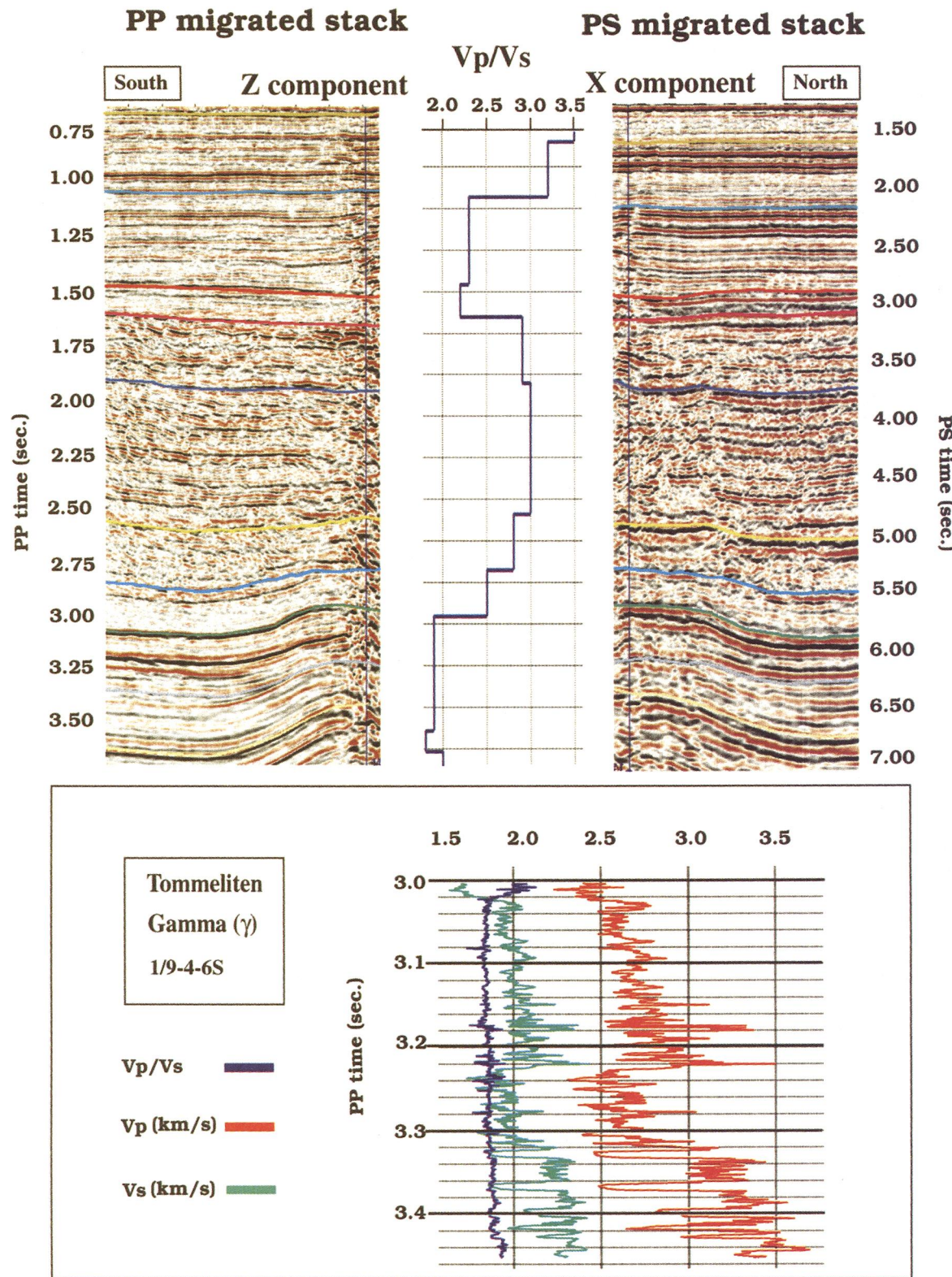


FIG. 9. The sections at the top left and top right show the correlation of seismic horizons between the X- and Z-components of the sea-floor data. The corresponding  $V_p/V_s$  ratio is shown in the middle. The P-wave velocity (red), S-wave velocity (green), and  $V_p/V_s$  ratio (blue) shown in the bottom part of the figure were obtained from well logs at the nearby Tommeliten Gamma structure.

*X*-component with the processed *Z*-component. Picking the same reflector on both sections allowed the compressional-to-shear-wave velocity ratio to be computed using the observed traveltimes. The final depth-dependent compressional-to-shear-wave velocity profile is shown in Figure 9. The profile is in accordance with a similar profile given by Dangerfield and Brown (1987) derived for a similar Tertiary sequence. Ratios of around 3.5 were found in the shallow, unconsolidated clays, while lower ratios were estimated in the consolidated shales down to approximately 1.5 s *PP* time. Below 1.5 s, unconsolidated gumbo-clays cause the ratio to increase up to approximately 3.0. For the Upper Cretaceous reservoirs, low compressional-to-shear-wave ratios around 1.8 are found. These reservoir values are in good agreement with compressional-to-shear-wave velocity ratios based on compressional- and shear-wave logs in a similar reservoir zone at the Gamma structure, 10 km to the north of the Alpha structure, shown in the bottom part of Figure 9.

The final *X*-component section is shown in Figure 10; Figure 11 compares the conventional 3-D data and the *X*-component. Note the striking image of the reflectors in the gas chimney area, as compared to the conventional 3-D section.

Since the image is based on processing of data containing the *PS* mode, one would expect the downgoing compressional wave to be attenuated when propagating through the gas chimney. This would seemingly prevent obtaining images of the quality shown in Figure 10. A possible explanation is that the *PS*-waves effectively undershoot the gas chimney, as illustrated in Figure 12. The thick red rays represent *PS*-waves where the downgoing compressional raypath is mainly outside the gas chimney and hence little affected by the gas in the sediments. The upgoing shear wave (green and dotted green raypaths), on the other hand, is traveling through the gas chimney but is largely unaffected by the presence of gas and reaches the sensors at the sea floor. However, when the downgoing compressional waves are propagating through the gas chimney, as shown by the red dotted raypaths, the influence of the gas in the sediments is substantial, and no significant amount of energy will reach the sensors at the sea floor.

It is by no means clear that the sections shown in Figure 10 represent a true image of the Tommeliten Alpha structure. Moreover, the fundamental assumptions in the processing of the data is that the subsurface consists of plane dipping layers. This could possibly lead to errors in the final image. A better

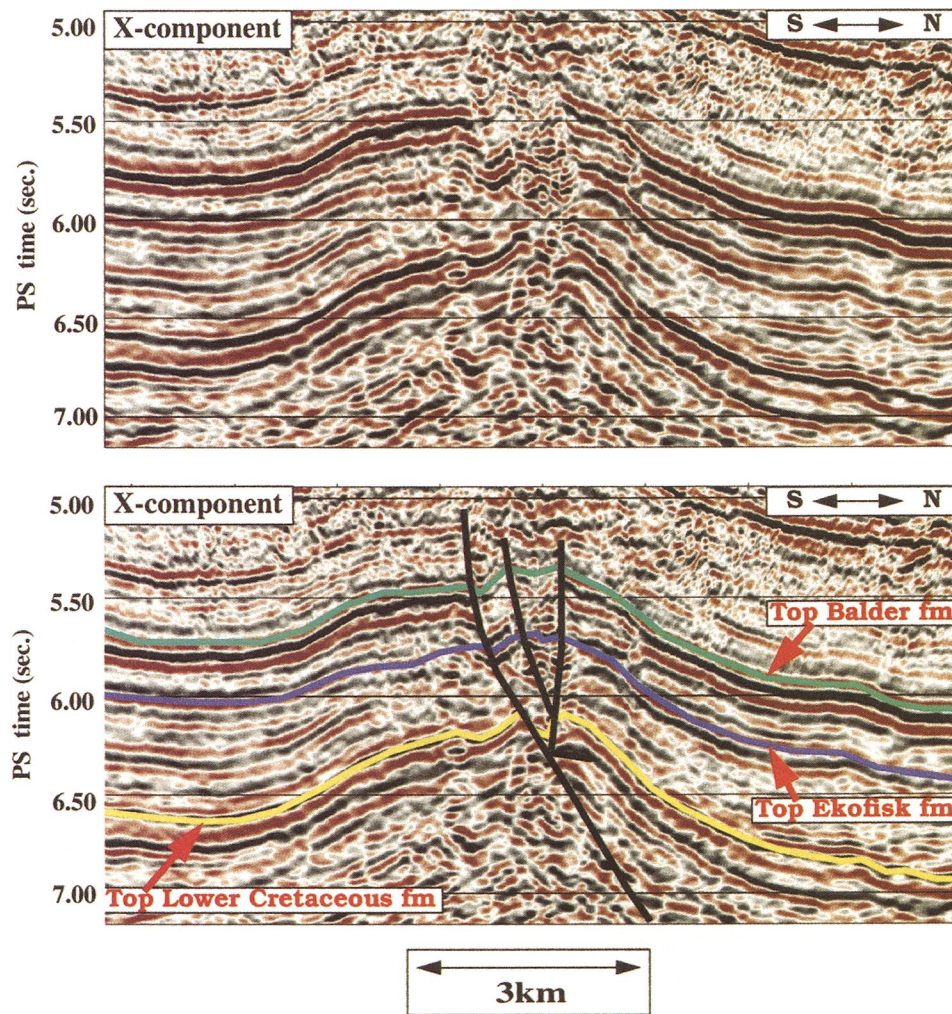


FIG. 10. Final migrated stack of the *X*-component with (bottom) and without (top) interpretation.

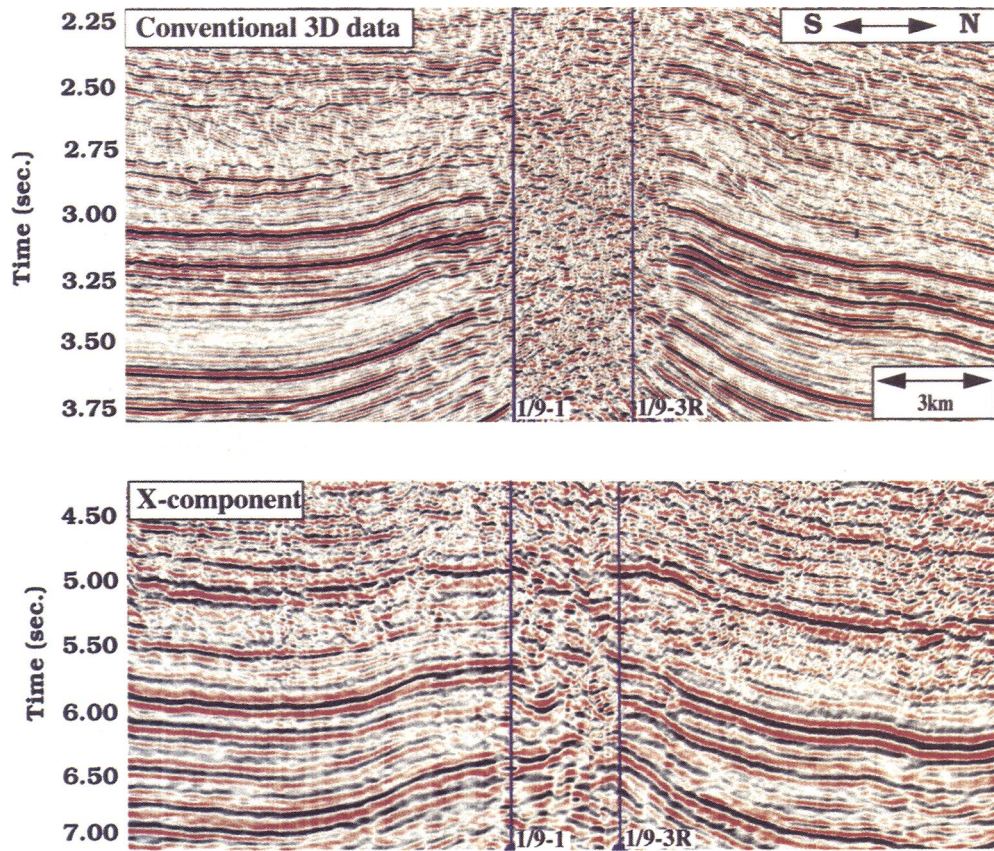


FIG. 11. Comparison between conventional 3-D data (top) and the  $X$ -component of the sea-floor data.

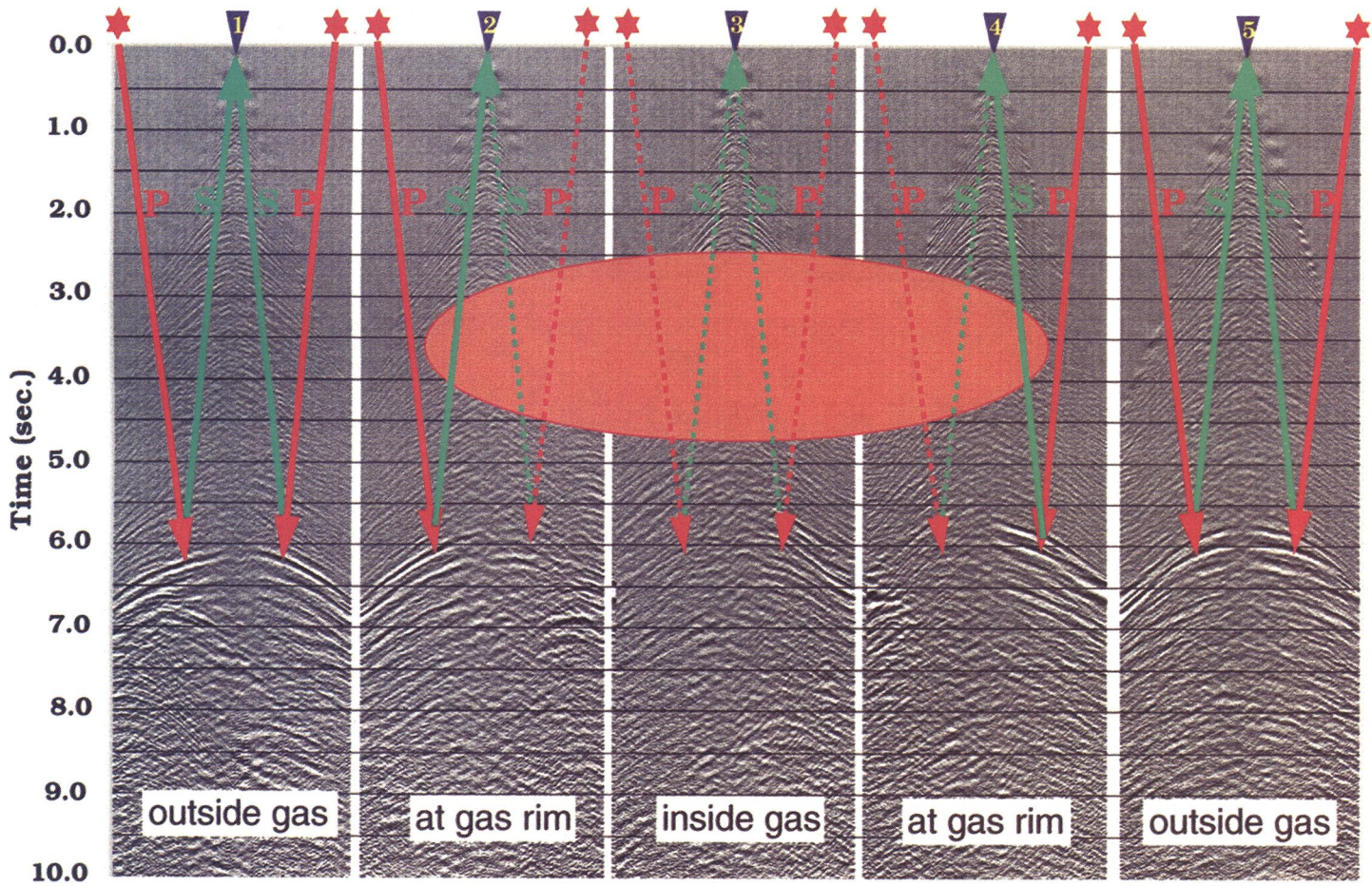


FIG. 12. Undershooting by  $PS$  rays of the Tommeliten Alpha structure.

approach to processing would be to use depth migration, where more general assumptions with respect to the subsurface could be made.

### INTERPRETATION

From the results shown above, it is clear that the *X*-component is our main information source for structural interpretation of the Cretaceous reservoirs at the crest of the Alpha structure. Comparing the *X*-component and *Z*-component sections as shown in Figures 7 and 9 and using the available well logs, the Balder, Ekofisk, and Cretaceous reflectors are identified on the *X*-component. Figure 10 shows the final image with and without structural interpretation. As is clearly seen, the area of uncertain structural interpretation has been significantly reduced, especially in the deeper parts of the section. It is now a wedge shape narrowing with depth. For Lower Cretaceous intervals, it is possible to follow the reflectors through the gas. For the Upper Cretaceous reservoirs, this wedge is still a little over 500 m wide.

The minor vertical time shifts of reflectors at the top of the structure clearly suggests that some faulting has taken place here. The interpreted fault pattern shown in Figure 10 is, however, one of several possibilities.

In essence a similar conclusion is reported by Berg et al. (1994a,b). The similarity, however, is coincidental since their *S*-wave processing was based on incorrect assumptions. Their resulting image did show very good reflector continuity through the gas zone, but the lack of structural tie with other data in the vicinity of the gas underlined a processing problem.

### CONCLUSIONS

*PS* converted wave data can be acquired successfully in a marine environment by using geophones buried into the sea floor. Processing marine *PS* converted data can be performed using well-known techniques borrowed from processing multicomponent land data. The final images and the interpretation of these show that converted waves can be used to image

through a gas chimney, where the quality of conventional compressional data is poor. The interpretation supports the idea that the Tommeliten Alpha structure is a faulted dome.

### ACKNOWLEDGMENTS

We particularly thank Eivind Berg, Bjørnar Svenning, James Martin, Mark Harrison, and Åsmund Sjøen Pedersen. We are grateful for the enduring patience and continued enthusiasm showed by Kåre Horpestad and Knut Georg Røssland, both with Statoil. We also thank Statoil, Fina, and Agip for permission to publish this work.

### REFERENCES

- Allnor, R., Caiti, A., and Arntsen, B., 1997, Inversion of seismic surface waves for shear wave velocities: 67th Ann. Internat. Mtg., Soc. Expl. Geophys., Expanded Abstracts, 1921–1924.
- Amundsen, L., and Reitan, A., 1995, Decomposition of multicomponent seafloor data into upgoing and downgoing *P*- and *S*-waves: *Geophysics*, **60**, 563–572.
- Berg, E., Svenning, B., and Martin, J., 1994a, SUMIC—A new strategic tool for exploration and reservoir mapping: 56th Ann. Mtg., Eur. Assn. Expl. Geophys., Expanded Abstracts, 653–656.
- , 1994b, SUMIC—Multicomponent sea-bottom seismic surveying in the North Sea—Data interpretation and applications: 54th Ann. Internat. Mtg., Soc. Expl. Geophys., Expanded Abstracts, 477–480.
- Dangerfield, J. A., 1992, Ekofisk field development: Making images of a gas obscured reservoir, in Sheriff, R. E., Ed., Reservoir geophysics: Soc. Expl. Geophys., 98–109.
- Dangerfield, J. A., and Brown, D. A., 1987, The Ekofisk field, in Kieppé, J., Berg, E. W., Buller, A. T., Hjelmeland, O., and Torsater, O., Eds., North Sea Oil and Gas Reservoirs: Graham and Trotman Ltd., 3–22.
- Harrison, M. P., 1992, Processing of *P-SV* surface-seismic data: Anisotropy analysis, dip moveout and migration: Ph.D. thesis, Univ. Calgary.
- Harrison, M., and Stewart, R., 1993, Poststack migration of *p-sv* seismic data: *Geophysics*, **58**, 1127–1135.
- Tessmer, G., and Behle, A., 1988, Common reflection point data-stacking technique for converted waves: *Geophys. Prosp.*, **36**, 661–668.
- Tessmer, G., Krajewski, P., Fertig, J., and Behle, A., 1990, Processing of *PS*-reflection data applying a common conversion-point stacking technique: *Geophys. Prosp.*, **36**, 661–668.
- White, J. E., 1975, Computed seismic speeds and attenuation in rocks with partial gas saturation: *Geophysics*, **40**, 224–232.